Impact of long-term salinity exposure in anaerobic membrane bioreactors treating phenolic wastewater

Performance robustness and endured microbial community

Muñoz Sierra, Julian D.; Oosterkamp, Margreet J.; Wang, Wei; Spanjers, H.; van Lier, Jules B.

DOI
10.1016/j.watres.2018.05.006

Publication date
2018

Document Version
Final published version

Published in
Water Research

Water Research 141 (2018) 172–184

Contents lists available at ScienceDirect

Water Research

journal homepage: www.elsevier.com/locate/watres

Impact of long-term salinity exposure in anaerobic membrane bioreactors treating phenolic wastewater: Performance robustness and endured microbial community

Julian D. Muñoz Sierra [a, *], Margreet J. Oosterkamp [a], Wei Wang [a, b], Henri Spanjers [a], Jules B. van Lier [a]

[a] Section Sanitary Engineering, Department of Water Management, Delft University of Technology, Stevinweg 1, 2628 CN, Delft, The Netherlands
[b] Department of Municipal Engineering, School of Civil and Hydraulic Engineering, Hefei University of Technology, Hefei 230009, China

ARTICLE INFO

Article history:
Received 24 January 2018
Received in revised form
12 April 2018
Accepted 5 May 2018
Available online 7 May 2018

Keywords:
AnMBR
Salinity
Phenol
Microbial community
Sodium
Wastewater treatment

ABSTRACT

Industrial wastewaters are becoming increasingly associated with extreme conditions such as the presence of refractory compounds and high salinity that adversely affect biomass retention or reduce biological activity. Hence, this study evaluated the impact of long-term salinity increase to 20 $gNa^{+}.L^{-1}$ on the bioconversion performance and microbial community composition in anaerobic membrane bioreactors treating phenolic wastewater. Phenol removal efficiency of up to 99.9% was achieved at 14 $gNa^{+}.L^{-1}$. Phenol conversion rates of 5.1 $mgPh.gVSS^{-1}.d^{-1}$, 4.7 $mgPh.gVSS^{-1}.d^{-1}$, and 11.7 $mgPh.gVSS^{-1}.d^{-1}$ were obtained at 16 $gNa^{+}.L^{-1}$,18 $gNa^{+}.L^{-1}$ and 20 $gNa^{+}.L^{-1}$, respectively. The AnMBR's performance was not affected by short-term step-wise salinity fluctuations of 2 $gNa^{+}.L^{-1}$ in the last phase of the experiment. It was also demonstrated in batch tests that the COD removal and methane production rate were higher at a K^{+}:Na^{+} ratio of 0.05, indicating the importance of potassium to maintain the methanogenic activity. The salinity increase adversely affected the transmembrane pressure likely due to a particle size decrease from 185 μm at 14 $gNa^{+}.L^{-1}$ to 16 μm at 20 $gNa^{+}.L^{-1}$. Microbial community was dominated by bacteria belonging to the *Clostridium* genus and archaea by *Methanobacterium* and *Methanosaeta* genus. Syntrophic phenol degraders, such as *Pelotomaculum* genus were found to be increased when the maximum phenol conversion rate was attained at 20 $gNa^{+}.L^{-1}$. Overall, the observed robustness of the AnMBR performance indicated an endured microbial community to salinity changes in the range of the sodium concentrations applied.

1. Introduction

Chemical, food processing, textile and petroleum industries are considered as the primary producers of saline wastewater (Ng et al., 2005; Yang et al., 2013). About 5% of these industrial effluents have saline or hypersaline characteristics (Lefebvre et al., 2007; Praveen et al., 2015). The degradation of a large variety of aromatic contaminants such as phenols and polyphenols remains as a challenge for industrial wastewater treatment, which often needs to be accomplished at high salinity.

Previous research indicated the potentials of adaptation of halotolerant microorganisms in anaerobic treatment processes to saline conditions (Lefebvre et al., 2007; Margesin and Schinner, 2001). Due to an osmotic pressure difference across the cell membrane, salt concentrations higher than 1% induce disintegration of cells because of plasmolysis and dehydration (Wood, 2015). As a result, a decrease in biodegradation and effluent quality are recognized as the most important consequences (Abou-Elela et al., 2010; Yogalakshmi and Joseph, 2010). Osmo-adaptation by producing or adding compatible solutes or accumulation of intracellular potassium could mitigate the loss on biomass activity due to pressure differences across the cell membrane caused by high salinity (Le Borgne et al., 2008; Vyrides and Stuckey, 2017).

High salinity, mainly resulting from sodium salts, has an adverse impact on the performance of anaerobic wastewater treatment systems due to an inhibitory effect of sodium and the disintegration of flocs leading to a prominent biomass washout (Ismail et al., 2008; Pevere et al., 2007; Vyrides and Stuckey, 2009a). In

* Corresponding author.
E-mail address: J.D.MunozSierra@tudelft.nl (J.D. Muñoz Sierra).

https://doi.org/10.1016/j.watres.2018.05.006

anaerobic high-rate reactors, retaining biomass such as by sludge granulation is essential for an efficient treatment (van Lier et al., 2015). Sludge granulation could be hampered at high salt concentrations as granule strength is considerably reduced when sodium replaces the calcium ions (Ismail et al., 2010; Jeison et al., 2008a). In contrast, because of the membrane filtration in anaerobic membrane bioreactors (AnMBRs), suspended biomass under highly saline conditions can be retained and enriched. This advantage of AnMBRs provides an opportunity for microorganisms to adapt to a wide range of sodium concentrations. However, several harmful effects of high salinity on anaerobic biodegradation of waste streams have been reported by previous studies (Muñoz Sierra et al., 2017; Song et al., 2016). Muñoz Sierra et al. (2017) found 50% inhibition of methanogenic activity at about 23 $gNa^{+}.L^{-1}$ and complete inhibition at about 34 $gNa^{+}.L^{-1}$. Song et al. (2016) showed that a salt concentration above 10 $gNaCl.L^{-1}$ reduced biogas production and COD removal in an AnMBR. Furthermore, the adaptation of microbial communities to an extended range of salinity enhances the opportunities for anaerobic biological wastewater treatment applications. Luo et al. (2016) demonstrated that acclimation to high salt concentration could lead to the succession of halotolerant or even halophilic microorganisms, thereby gradually recovering the bioreactor performance. Sudmalis et al. (2018) indicated that increase in salinity results in a shift in the bacterial and hydrogenotrophic methanogens populations. Archaea abundance and the genes involved in methanogenesis decrease significantly when salinity increases from low to high levels; likewise, the gene abundance in the hydrogenotrophic pathway is lower (Wu et al., 2017). Correspondingly, acetoclastic methanogens show a higher resistance to high salinity than hydrogenotrophic methanogens (Wang et al., 2017a).

However, studies that have reported the performance of AnMBRs during long-term continuous operation at high salinity are few and limited; especially there is none for the degradation of phenolic compounds. The studies focused either on the treatment of saline acidified wastewater (6–24 $gNa^{+}.L^{-1}$) (Jeison et al., 2008b), or protein containing saline wastewater (25 $gNa^{+}.L^{-1}$) (Hemmelmann et al., 2013). On the other hand, other studies give attention to municipal wastewater (Vyrides and Stuckey, 2009b), the removal of specific trace organic contaminants (0–15 $gNaCl.L^{-1}$) (Song et al., 2016) and the contribution to membrane fouling when operating an AnMBR under saline conditions (35 $gNaCl.L^{-1}$) (Vyrides and Stuckey, 2011). Also, the use of forward osmosis-AnMBRs with transient salinity build-up has been explored (Chen et al., 2014).

The COD of chemical wastewater dissipates little energy during its breakdown, leading to low biomass yield and thus long or even infinite sludge retention times. The latter is a striking advantage for AnMBRs since there is no sludge wash-out giving the chance to enrich salt tolerant biomass or even halophilic species able to degrade a model aromatic compound as phenol. Previous research on microbial community structure and dynamics under high salinity conditions have focused specifically on digesters (De Vrieze et al., 2017) and UASB reactors (Gagliano et al., 2017; Wang et al., 2017b), but there is no insight into the response of the retained biomass in an AnMBR to long-term high salinity exposure with phenolic wastewaters. Therefore, further research is required that will advance the understanding to successful application of AnMBRs for the treatment of chemical wastewaters under extreme conditions such as high salinity conditions. In view of the above, this study aims to evaluate the phenol bioconversion performance and microbial community dynamics in long-term operation of an AnMBR in response to a stepwise increase in sodium concentration. Six phases of operation were established to investigate whether the changes in sodium concentrations affected the membrane filtration behavior, biomass particle size, methanogenic activity, microbial diversity and phenol degraders abundance. The effect of K^{+}:Na^{+} concentration ratio on phenol and COD bioconversion at high salinity was assessed in batch tests.

2. Materials and methods

2.1. Experimental set-up and operation

The experiments were carried out using a laboratory scale AnMBR reactor with an effective volume of 6.5 L, equipped with an ultra-filtration (UF) side-stream membrane module (Fig. 1.). The average sludge retention time (SRT) was kept at about 40.0 ± 2.0 days. A tubular PVDF membrane (Pentair, The Netherlands) with 5.5 mm inner diameter, 30 nm pore size, and 0.64 m length was used. The experimental set-up was equipped with feed, recycle and effluent pumps (Watson-Marlow 120U/DV, 220Du), temperature and pH sensors (Endress & Hauser, Memosens), and a biogas flowmeter (Ritter, Milligas Counter MGC-1 PMMA, Germany). Transmembrane pressure (TMP) was measured by three pressure sensors (AE Sensors ATM, The Netherlands). The temperature of the reactor was controlled by a thermostatic water bath (Tamson Instruments, The Netherlands). The system was monitored by a computer running LabView software (version 15.0.1f1, National Instruments, USA). The AnMBR was inoculated with mesophilic anaerobic biomass obtained from a full-scale UASB reactor treating industrial wastewater (Shell, Moerdijk, The Netherlands). The initial concentration of volatile suspended solids (VSS) and total suspended solids (TSS) were 20.1 $g\,L^{-1}$ and 50.9 $g\,L^{-1}$, respectively.

The synthetic wastewater consisted of sodium acetate ($C_2H_3NaO_2$) and phenol (C_6H_6O) with varying concentrations depending on reactor operational conditions. The amount of sodium chloride (NaCl), and solutions of K_2HPO_4 (34.85 gL^{-1}) and NaH_2PO_4 (24 $g\,L^{-1}$) varied according to the sodium concentration applied in the reactor maintaining a fixed K^{+}:Na^{+} ratio of 0.05. Yeast extract (0.5 $g.L^{-1}$), macronutrients (9 $mL.L^{-1}$), and micronutrients (4.5 $mL.L^{-1}$) were supplemented. Macronutrients solution included (in $g.L^{-1}$): NH_4Cl 170, $CaCl_2.2H_2O$ 8, and $MgSO_4.7H_2O$ 9; and micronutrients solution contained (in $g.L^{-1}$): $FeCl_3.6H_2O$ 2, $CoCl_2.6H_2O$ 2, $MnCl_2.4H_2O$ 0.5, $CuCl_2.2H_2O$ 0.03, $ZnCl_2$ 0.05, H_3BO_3 0.05, $(NH_4)_6Mo_7O_2.4H_2O$ 0.09, Na_2SeO_3 0.1, $NiCl_2.6H_2O$ 0.05, EDTA 1, Na_2WO_4 0.08 (Muñoz Sierra et al., 2017). The influent concentration of phenol was gradually increased to 0.5 $g.L^{-1}$ as indicated in Fig. 2A. Moreover, the sodium concentrations in the reactor were increased from 8 to 20 $gNa^{+}.L^{-1}$ by long-term and short-term exposures in six phases. In phase I, the salinity rise in the AnMBR occurred starting at 8 $gNa^{+}.L^{-1}$ and then to 10 $gNa^{+}.L^{-1}$ with exposures of about 20 days each. Long-term (phases II-IV) exposure was carried out for 112 days at 14 $gNa^{+}.L^{-1}$, 24 days at 18 $gNa^{+}.L^{-1}$, and 133 days at 16 $gNa^{+}.L^{-1}$. Short-term salinity exposure cycles (phases V and VI) of 40 days were carried out at the end of the long-term operation, first by a step-wise increase from 16 to 19 $gNa^{+}.L^{-1}$ and second by a step-wise increase/decrease from 18 to 20 $gNa^{+}.L^{-1}$. The AnMBR was operated during 391 days under mesophilic condition (35.0 ± 1.4 °C). The operational conditions during all phases are shown in Table 1. In this study, the term high salinity refers to the high concentration of sodium in the water.

2.2. K^{+}:Na^{+} ratio effect on bioconversion through batch tests

Biomass samples from the AnMBR were taken, and two batch tests were conducted at the end of the phase IV and phase VI. 500 mL anaerobic bottles at sodium concentrations of 16, 20 and 24 $gNa^{+}.L^{-1}$ were used to assess the K^{+}:Na^{+} concentration ratio effect on the bioconversion. Temperature and mixing were controlled in a

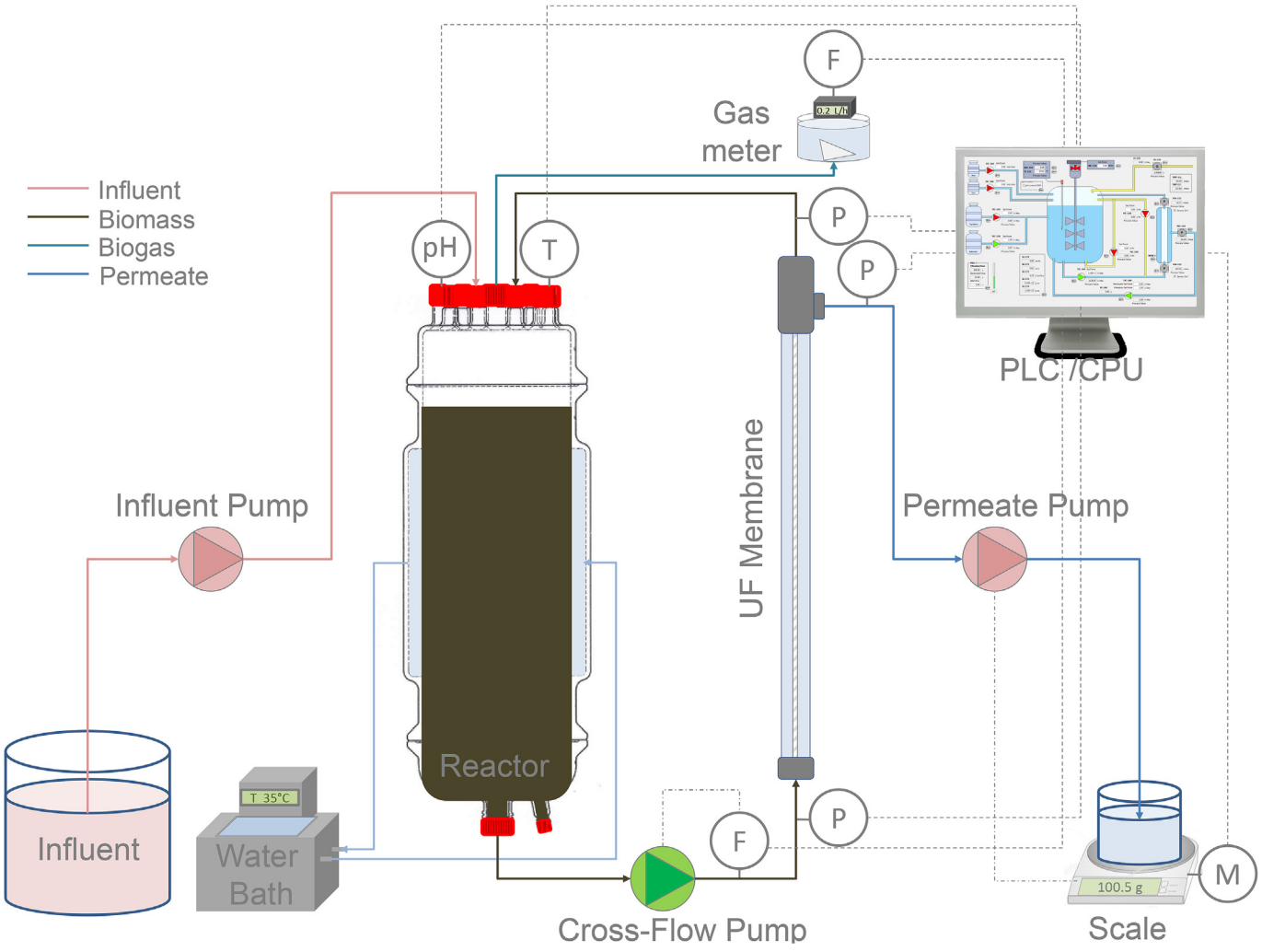

Fig. 1. Schematic illustration of AnMBR setup.

Table 1
Operational conditions of the AnMBR.

Day	Salinity [$gNa^{+}.L^{-1}$]	OLR [$gCOD.L^{-1}.d^{-1}$]	Phenol loading rate [$mgPh.L^{-1}.d^{-1}$]	VSS [$gVSS.L^{-1}$]	Phase
0	8	0.15	0.77	30.87	I
30	10	1.54	0.77	14.15	
100	14	3.06	12.85	19.19	II
128	14	3.08	15.38	16.15	
148	14	3.12	30.77	17.75	
157	18	3.12	38.46	17.75	III
178	18	3.12	38.46	8.16	
221	16	5.45	67.23	12.78	IV
280	16	3.12	38.46	9.26	
311	16	3.12	38.46	16.93	
350	19	6.24	76.92	13.50	V
382	20	6.24	76.92	9.70	VI

shaker at 35 °C and 120 rpm respectively. The first test, at the end of phase IV, was carried out maintaining the K^{+}:Na^{+} ratio at 0.05 while keeping the above concentrations of sodium. In the second test, the K^{+} concentration was kept constant for all sodium concentrations (see Table 2.). The K^{+}:Na^{+} ratios tested were 0.05, 0.03, 0.025 and 0.002. Four consecutive feedings of the substrate (acetate and phenol) were applied. Initial COD and phenol concentrations were 3.5 $g.L^{-1}$ and 50 $mgPh.L^{-1}$, respectively. Methane production rate was recorded by an AMPTS device (Bioprocess Control, Sweden).

2.3. Microbial community and statistical analysis

Biomass samples were taken from the AnMBR in all phases to

Table 2
K^+, Na^+ concentrations and K^+:Na^+ ratios used in batch tests.

	1st Batch			2nd Batch		
$gK^+.L^{-1}$	0.8	1	1.2	0.5	0.5	0.5
$gNa^+.L^{-1}$	16	20	24	16	20	24
K^+:Na^+	0.05	0.05	0.05	0.03	0.025	0.02

evaluate the microbial community dynamics. The DNeasy Ultra-Clean Microbial kit (Qiagen, Hilden, Germany) was used to extract DNA from 0.5 g of biomass. The quality and quantity of the DNA obtained was checked by agarose gel electrophoresis and Qubit3.0 DNA detection (Qubit® dsDNA HS Assay Kit, Life Technologies, U.S.), respectively. High throughput sequencing was performed by using the MiSeq Illumina platform and primers for bacterial and archaeal (V3-V4) 16S rRNA genes (BaseClear, Leiden, the Netherlands). The QIIME pipeline (version 1.9.0) was used to analyze the sequences (Caporaso et al., 2010). Demultiplexing and quality filtering were performed with parameter values $Q = 20$, $r = 3$, and $p = 0.75$. Chimeric sequences were removed using UCHIME2 (version 9.0) algorithm (Edgar, 2016). Sequences were clustered into operational taxonomic units (OTUs) with a 97% similarity as the cutoff, with UCLUST algorithm (Edgar, 2010). Singletons were removed, and OTUs with an occurrence less than three times in at least one sample were excluded. Taxonomic assignation was performed using the Silva database (SILVA-128) with UCLUST (McDonald et al., 2012). Alpha diversity was determined after random subsampling using the metrics Chao1, observed OTUs and Faith's phylogenetic distance in QUIIME. For beta diversity, separate non-metric distance scaling (NMDS) and PCoA analysis of the microbial community were made based on the unweighted Unifrac distance measure. Both alpha and beta diversity plots were generated with the phyloseq (McMurdie and Holmes, 2013) and ggplot2 packages in the R environment. Sequences have been submitted and assigned the number SRP128989.

2.4. Analytical techniques

2.4.1. Particle size distribution

Measurement of particle size distribution (PSD) was carried out by using a DIPA-2000 EyeTech™ particle analyzer (Donner Technologies, Or Akiva, Israel) with an A100 and B100 laser lens (measuring range 0.1–300 μm and 1–2000 μm, respectively) and a liquid flow cell DCM-104A (10 × 10 mm).

2.4.2. Flow cytometry assay

Flow cytometry (FCM) assay was conducted to determine the quality of the biomass samples after sodium concentration changes between phase II, III and IV, and significant volatile suspended solids reduction. BD Accuri C6® flow cytometer (BD Accuri cytometers, Belgium) was used, with a 50 mW laser emitting at a fixed wavelength of 488 nm. BD Accuri CFlow® software was used for data processing of cells with intact and compromised membranes. Biomass samples were diluted (to obtain bacterial concentration less than 2×10^5 cells mL^{-1}), stained (live/dead) and evaluated following the protocol defined by Prest et al. (2013).

2.4.3. Specific methanogenic activity (SMA) and biogas content

SMA tests were performed in triplicate using an automated methane potential test system (AMPTS, Bioprocess Control, Sweden) and were carried out at 35 °C. The ratio K^+:Na^+ was kept constant at 0.05 in the media. The initial pH was adjusted to 7.0 (20 ± 0.4 °C). Methane content of the biogas was analyzed using a gas chromatograph 7890A (GC) system (Agilent Technologies, US) equipped with a flame ionization detector. The temperatures of the oven, front inlet, and front detector were 45 °C, 200 °C, and 200 °C, respectively.

2.4.4. Other analytical methods

Hach Lange kits were used to measure chemical oxygen demand (COD). The COD was measured using a VIS - spectrophotometer (DR3900, Hach Lange, Germany). Phenol concentration was measured by Merck – Spectroquant® Phenol cell kits using a spectrophotometer NOVA60 (Merck, Germany). Phenol concentrations were double-checked using a high-pressure liquid chromatography HPLC LC-20AT (Shimadzu, Japan) equipped with a 4.6 mm reversed phase C18 column (Phenomenex, The Netherlands) and a UV detector at a wavelength of 280 nm. The solvent used was 25% (v/v) acetonitrile as mobile phase at a flow rate of 0.95 $mL.min^{-1}$. The column oven was set at 30 °C. Sodium concentrations in the reactor were measured by Ion Chromatography (Metrohm, Switzerland). Dilutions were applied to samples and were prepared in triplicates. Calibration curves were made using AAS standard solution (Sigma-Aldrich) in the range between 0.1 and 50 ppm. The final concentrations were calculated by using the MagIC Net 3.2 software.

3. Results and discussion

3.1. AnMBR process performance

Phenol, COD, and sodium concentrations of the influent were controlled and monitored during the operation of the AnMBR (Fig. 2. A). During phase I, COD and phenol removal efficiency varied from 83.8% to 98.6% and 0–77.0%, respectively (Fig. 2. B, C). The performance of the reactor was unstable, coinciding with the acclimation of biomass to the operational conditions, when sodium concentration was increased from 8 $gNa^+.L^{-1}$ to 14 $gNa^+.L^{-1}$ and organic loading rate was increased from 0.2 $gCOD.L^{-1}.d^{-1}$ to 3.1 $gCOD.L^{-1}.d^{-1}$. The influent phenol concentration was increased from 10 to 100 $mgPh.L^{-1}$ at the end of this phase. The maximum conversion rates achieved under the aforementioned conditions were 2.9 $mgPh.L^{-1}.d^{-1}$ (0.2 $mgPh.gVSS^{-1}.d^{-1}$) and 3.0 $gCOD.L^{-1}.d^{-1}$ (0.2 $gCOD.gVSS^{-1}.d^{-1}$). Biogas production rate gradually increased by raising the OLR in accordance with the expected methane production (Fig. S1). In phase II, when influent phenol concentration was increased from 100 to 500 mg L^{-1}, a phenol removal efficiency of up to 99.9% was achieved (Fig. 2. C). Better stability of the AnMBR and higher phenol conversion rates than in phase I were observed; in phase II the sodium concentration was kept constant at 14 $gNa^+.L^{-1}$. The phenol conversion rate increased with 88% to 30.8 $mgPh.L^{-1}.d^{-1}$ (1.7 $mgPh.gVSS^{-1}.d^{-1}$), indicating that the applied constant salt concentration was beneficial for developing a stable microbial conversion process, enhancing the phenol uptake. Similarly, Wang et al. (2017b) reported that a constant sodium concentration of 10 $gNa^+.L^{-1}$ resulted in stable biomass activities of the phenolics degraders and methanogens at influent total phenols (phenol, catechol, resorcinol and hydroquinone) concentrations in the range of 100–500 $mg.L^{-1}$. Moreover, Poirier et al. (2016) inferred that the stability of the anaerobic digestion process is reduced by

phenol concentrations above concentrations of 1 gPh.L^{-1}, and therefore the impact on phenol biodegradation might be attributed mainly to the salinity changes in this case.

At the beginning of phase III, a one-step salinity increase of 4 gNa^+.L^{-1} (from 14 to 18 gNa^+.L^{-1}) was applied. Phenol and COD removal efficiencies decreased at the end of this phase with COD values in the permeate of about 1.29 gCOD.L^{-1}. The volatile suspended solids (VSS) concentration remarkably decreased by 54% (Table 1.), and higher biogas production was observed around day 170.

An average phenol conversion rate of 38.4 mgPh.L^{-1}.d^{-1} was achieved at 18 gNa^+.L^{-1}. However, the phenol conversion rate varied between 2.2 mgPh.gVSS^{-1}.d^{-1} and 4.7 mgPh.gVSS^{-1}.d^{-1}. Interestingly, flow cytometry (FCM) results indicated a 21.2% increase in the number of cells with compromised membranes, when salinity increased from 14 to 18 gNa^+.L^{-1} (Table 3.). FCM results inferred that the quality of the biomass was reduced after this one-step increase of 4 gNa^+.L^{-1}. The rise in number of cells with compromised membranes could be attributed to the fact that microbial cultures are sensitive and exhibit limited adaptation to changes in ionic strength (Woolard and Irvine, 1995).

In phase IV, the sodium concentration was reduced to 16 gNa^+.L^{-1} to alleviate the negative effect observed in phase III. An additional 5.3% of cells with compromised membranes was observed with this salinity reduction, compared to the previous phase, reaching a total of 48.5% and 51.5% of cells with compromised and intact membranes, respectively (Table 3.). Because of the observed increased phenol concentration of about 67 mgPh.L^{-1} in the reactor permeate, the OLR was temporarily reduced to prevent phenol toxicity. Instability of the reactor was observed for about 85 days, and COD permeate concentration increased up to 1.14 gCOD.L^{-1} (Fig. 2. B). Phenol and COD conversion rates of 65.1 mgPh.L^{-1}.d^{-1} (5.1 mgPh.gVSS^{-1}.d^{-1}) and 5.4 gCOD.L^{-1}.d^{-1} (0.4 gCOD.gVSS^{-1}.d^{-1}) were observed, respectively. Praveen et al. (2015) showed that once a microbial community is acclimated to a certain salt concentration, the adaptation can become quickly lost if salinity is changed. However, the AnMBR COD conversion performance was not highly affected by a step-wise increase to 19 gNa^+.L^{-1} in phase V, neither by the salinity step-wise increases and decreases in phase VI. OLR was increased to 6.2 gCOD.L^{-1}.d^{-1} at the beginning of phase V. In these periods, the average phenol conversion rates were 113.0 mgPh.L^{-1}.d^{-1} (8.4 mgPh.gVSS^{-1}.d^{-1}) during phase V and 113.3 mgPh.L^{-1}.d^{-1} (11.7 mgPh.gVSS^{-1}.d^{-1}) at VI. The phenol and COD effluent concentration fluctuated to some extent by each sodium concentration change between 18 and 20 gNa^+.L^{-1}. That is in contrast to what was observed by Aslan and Şekerdağ (2016), who indicated that the COD removal significantly decreased at about 20 gNa^+.L^{-1} when treating saline wastewater in a UASB reactor. Our results demonstrated that a short-term continuous fluctuation between 18 and 20 gNa^+.L^{-1} eventually has no impact on the bioconversion anymore after a long-term operation, suggesting a successful gradual adaptation to higher sodium concentrations. As Carballa et al. (2015) inferred, a step-wise adaptation of the microbial community to stressful environmental conditions results in a strengthened microbiome against upcoming disturbances. In our current research, the salinity changes resulted in an endured microbial community increasing the process performance robustness in the range of sodium concentrations applied.

The methane production rate was more prone to variations during these last two phases. The specific methanogenic activities (SMA) obtained along the long-term operation of the AnMBR at the different sodium concentrations (see Table 4) decreased with 24% when salinity was increased from 14 gNa^+.L^{-1} to 20 gNa^+.L^{-1}. Nevertheless, the SMA of 0.55 ± 0.00 gCOD-CH_4.gVSS^{-1}.d^{-1} at 14 gNa^+.L^{-1} and 0.42 ± 0.22 gCOD-CH_4.gVSS^{-1}.d^{-1} at 20 gNa^+.L^{-1}, remained relatively high, which confirmed the adaptation of the methanogenic population to the salinity levels applied after long-term operation of the AnMBR. Earlier studies reported SMAs of biomass treating phenolic wastewater in a range from 0.15 to 0.66 gCOD-CH_4.gVSS^{-1}.d^{-1} (Hussain and Dubey, 2014; Wang et al., 2017d). The obtained SMA was higher than in other studies, applying sodium concentrations in the range of 0–20 gNa^+.L^{-1} (Jeison et al., 2008a; Muñoz Sierra et al., 2017), which might be attributed to the long-term acclimation of the biomass.

3.2. AnMBR membrane filtration performance

Transmembrane pressure (TMP) was lower than 150 mbar during the phases I to III at a flux of 2.0 L.m^{-2}.h^{-1} (Fig. 3.). This relatively low TMP is attributed to operation below the critical flux. However, the TMP was negatively affected by the salt concentration changes in phases III and IV and increased to 350 mbar in phases V and VI at a flux of 4.0 L.m^{-2}.h^{-1}. During these phases, the membrane filtration resistance increased from about 6.0×10^{12} m^{-1} to 28.0×10^{12} m^{-1}. The deterioration of membrane filtration performance was attributed to the observed decrease in biomass particle size when salinity was increased (see Fig. 3. B.). Likely, the low particle size had a significant influence on the cake layer compaction that increased the operational values of the filtration resistance (Hemmelmann et al., 2013). The median particle size decreased from 185 μm at 14 gNa^+.L^{-1} to 91 μm at 18 gNa^+.L^{-1} in phase III and to 56 μm at 16 gNa^+.L^{-1} in phase IV. The median biomass particle size was 35 μm at 19 gNa^+.L^{-1} and 16 μm at 20 gNa^+.L^{-1} meaning a ten-fold decrease following the long-term salinity exposure. TMP and membrane filtration resistance fluctuated especially during the salinity changes in phases V and VI. Possibly, in addition to the reduction in particle size, there were more biomass properties affected by salinity that contributed to a fluctuating membrane filtration resistance. For example, Yang et al. (2014) concluded that high sodium concentrations promote a compact gel layer formation. Similarly, Yurtsever et al. (2016) indicated that salinity induced large molecules, to be detected as foulants in gel/cake layer, may originate from biomass loosely bound extracellular polymeric substances.

3.3. K^+:Na^+ ratio effect on bioconversion

Since the intracellular ionic concentration of anaerobic microorganisms needs to be balanced with the environment, the K^+:Na^+ concentration ratio in the medium was assessed to identify its effect on bioconversion at high salinity. Biomass was taken from the AnMBR at the end of phase IV. Observed COD and phenol concentrations at 16, 20 and 24 gNa^+.L^{-1} under a fixed ratio K^+:Na^+ of 0.05 are depicted in Fig. 4. A, B and C. About 93.6% COD removal and 99.9% phenol removal was found at 16 gNa^+.L^{-1}. The lowest total COD concentration was about 207 mgCOD.L^{-1} at the end of the 2nd feed. At 20 gNa^+.L^{-1} and 24 gNa^+.L^{-1}, about 91.6% and 89.6% COD removal was achieved within all feedings, respectively, whereas 39% and 25% of phenol removal were observed. At 20 gNa^+.L^{-1}, the lowest phenol concentration was about 9 mgPh.L^{-1} at the end of the 1st feed, and the lowest COD concentration was 248.8 mgCOD.L^{-1} in the 4th feed. At 24 gNa^+.L^{-1} the lowest COD and phenol concentrations were 319 mgCOD.L^{-1} and 21 mgPh.L^{-1}, respectively. After the 2nd feed, a decrease in phenol degradation was detected for all tests, most probably because of phenol accumulation in subsequent feeding meaning a higher initial concentration that possibly leads to inhibition. The maximum methane production rates at 16, 20, and 24 gNa^+.L^{-1} were 0.16 ± 0.01, 0.13 ± 0.03, 0.09 ± 0.02 LCH_4.d^{-1}, respectively, inferring the

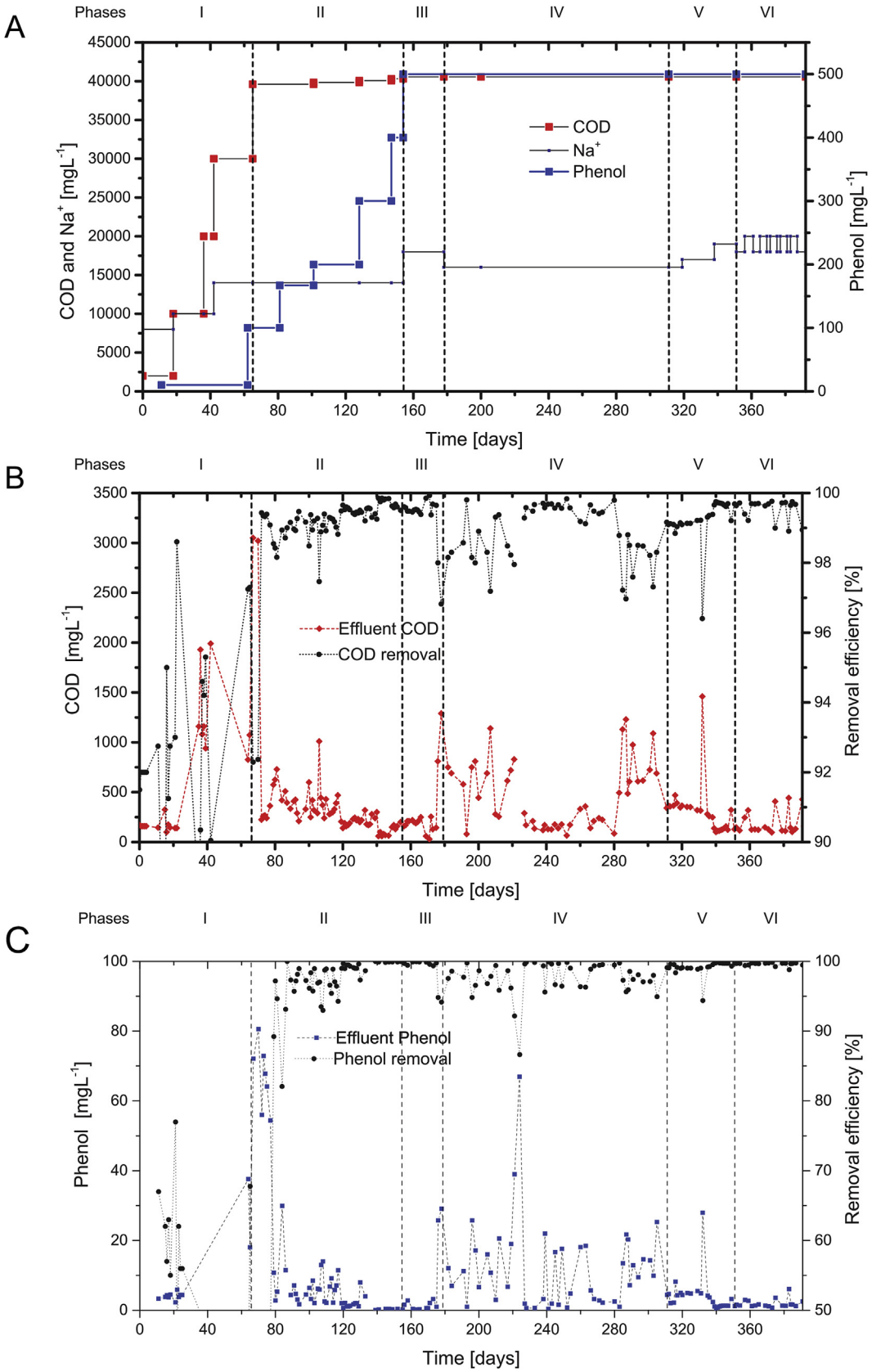

Fig. 2. A. Influent COD and Phenol, and reactor sodium concentrations. B. Permeate COD concentration and COD removal efficiency. C. Permeate phenol concentration and phenol removal efficiency.

Table 3
Cells with compromised and intact membranes after different sodium concentrations exposure.

[$gNa^{+}.L^{-1}$] in AnMBR	Compromised membranes [%]	Intact membranes [%]
14	22.1	77.9
18	43.3	56.7
16	48.5	51.5

Table 4
Specific methanogenic activities at different sodium concentrations in the AnMBR.

Salinity [$gNa^{+}.L^{-1}$]	SMA [$gCOD\text{-}CH_4.gVSS^{-1}d^{-1}$]	Phase
14	0.55 ± 0.00	II
18	0.64 ± 0.03	III
16	0.54 ± 0.02	IV
19	0.43 ± 0.05	V
20	0.42 ± 0.22	VI

negative impact of increasing sodium on methanogenic activity.

At the end of phase VI, batch tests were carried out at K^{+}:Na^{+} ratios of 0.03, 0.025 and 0.02 corresponding to 16, 20, 24 $gNa^{+}.L^{-1}$, respectively. The corresponding results are depicted in Fig. 4 D, E and F. At 16 $gNa^{+}.L^{-1}$, COD and phenol removals were 96.6% and 96.8%, respectively. Phenol was degraded completely at the end of the feed 1 to 3 at 20 and 24 $gNa^{+}.L^{-1}$, but the degradation lasted longer than in the previous batch. At 20 $gNa^{+}.L^{-1}$, 99% phenol removal was observed during the first feed and complete removal in the others. At 24 $gNa^{+}.L^{-1}$, an average of 82.7% COD removal and 94.4% phenol removal were found. The lowest COD concentrations obtained were 56 $mg.L^{-1}$, 118 $mg.L^{-1}$ and 179 $mg.L^{-1}$ at 16, 20, and 24 $gNa^{+}.L^{-1}$, respectively. It is inferred that in bacteria K^{+} allows the adaptation to environmental and metabolic changes (Kuo et al., 2005). Thereby, the improvement of phenol degradation might be attributed to the adaptation of biomass after it has been exposed to higher salinities of up to 20 $gNa^{+}.L^{-1}$ in phases V and VI. Methane

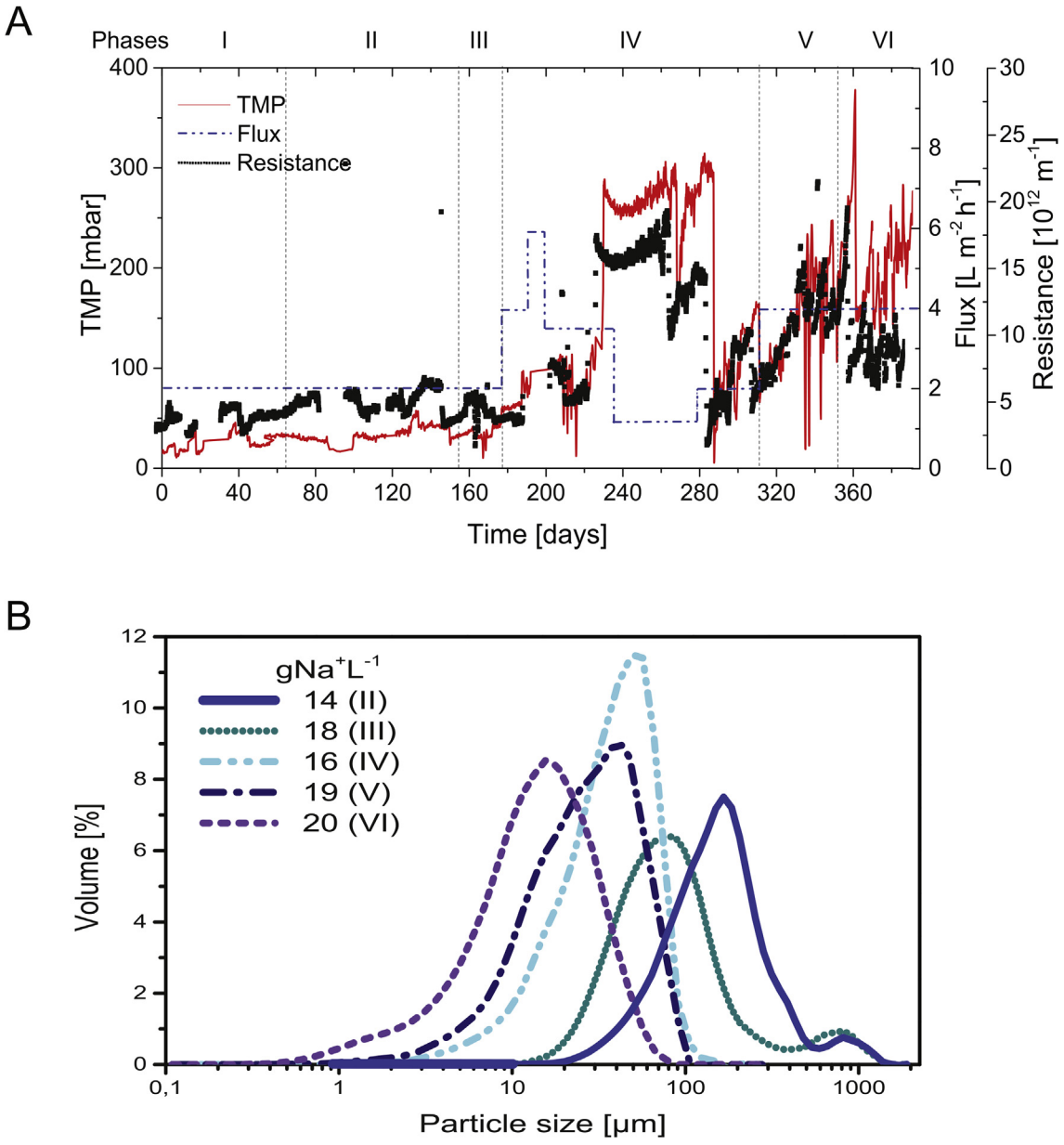

Fig. 3. A. Membrane Filtration performance. B. Biomass particle size distribution at different sodium concentrations.

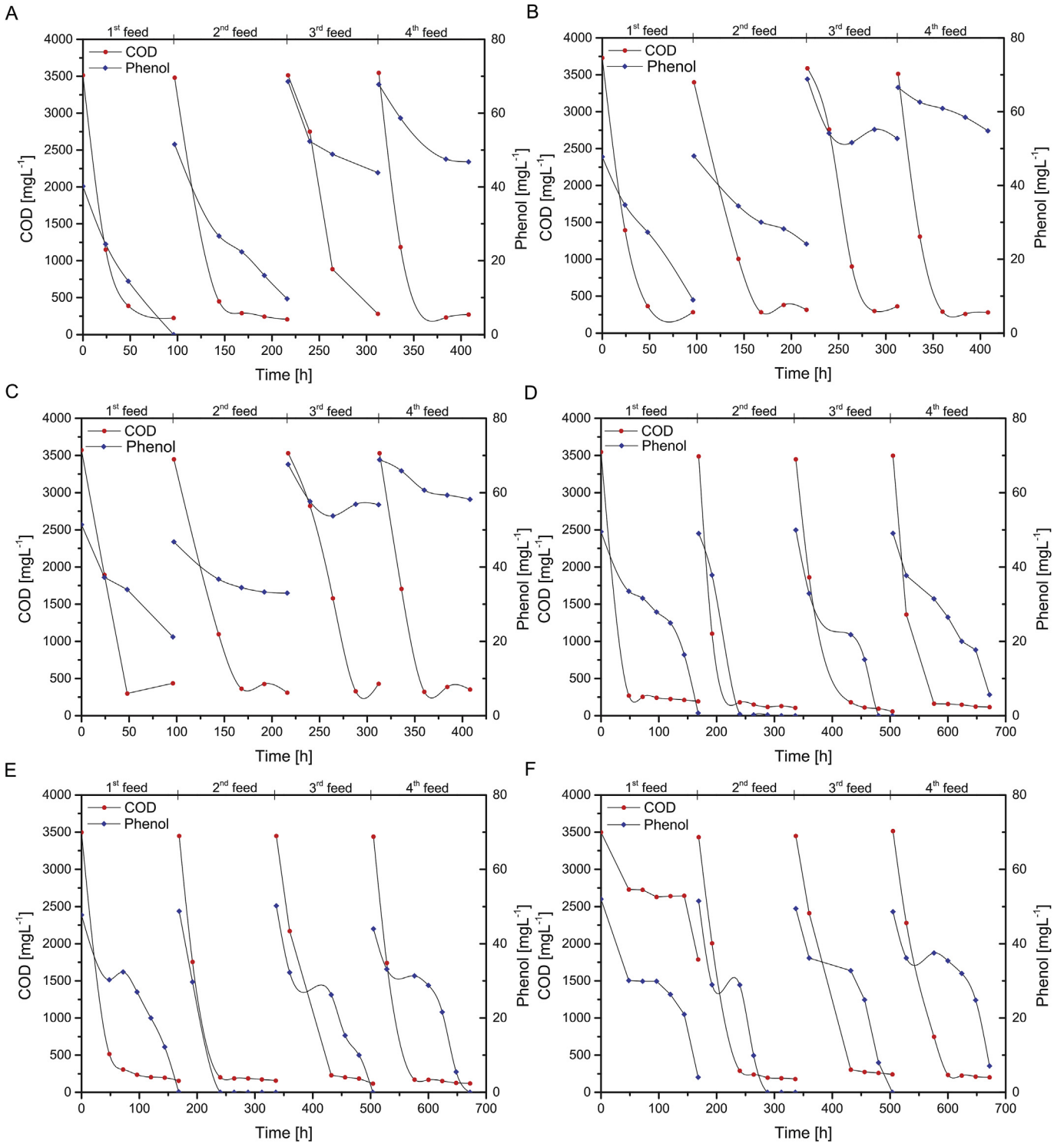

Fig. 4. Batch test assessment of impact of K^+:Na^+ ratio on COD and Phenol degradation. Constant K^+:Na^+ ratio of 0.05 A. 16 $gNa^+.L^{-1}$ (0.05) B. 20 $gNa^+.L^{-1}$ (0.05) and C. 24 $gNa^+.L^{-1}$(0.05). Varying K^+:Na^+ ratio D. 16 $gNa^+.L^{-1}$ (0.03). E. 20 $gNa^+.L^{-1}$(0.025) and F. 24 $gNa^+.L^{-1}$(0.02).

production rates average values of 0.13 ± 0.01, 0.11 ± 0.01, and 0.07 ± 0.02 $LCH_4.d^{-1}$ were observed at 16, 20 and 24 $gNa^+.L^{-1}$, respectively. Although the biomass could degrade phenol successfully, the COD removal and methane production rates for the 0.03, 0.025, and 0.02 K^+:Na^+ ratios were found to be lower than for the 0.05 K^+:Na^+ ratio. The latter seems to agree with the evidence that halophilic archaea use the salt-in strategy accumulating high intracellular concentrations of K^+ to balance and stabilize enzymes, being apparently more favorable for archaea than for bacteria (Le Borgne et al., 2008). This fact highlights the importance of K^+ for the archaea to preserve the methanogenic activity under saline conditions. Gagliano et al. (2017) found that a potassium concentration of 0.7 $gK^+.L^{-1}$ alleviates the negative effect of 20 $gNa^+.L^{-1}$ in a UASB. In both batch tests, the COD and phenol removal efficiency

were lower at 24 $gNa^{+}.L^{-1}$ compared to 16 and 20 $gNa^{+}.L^{-1}$.

Our current results confirmed the adverse impact of high sodium concentration on biomass activity as demonstrated by Muñoz Sierra et al. (2017). However, due to the long-term operation of the AnMBR at high salinity and adaptation of the microbial community to high sodium concentrations, this negative impact could be overcome. Further research should look at the effects of larger short-term random salinity fluctuations on the AnMBR phenol bioconversion and biomass properties analogous to treating actual industrial chemical wastewaters where such fluctuations can be expected.

3.4. Microbial community structure and dynamics

Based on the sequences from all biomass samples, 930 OTUs were identified of which 835 belonged to the bacteria and 95 to the archaea domain.

In the start-up phase I, the reactor performance was unstable (Fig. 2). Alpha diversity increased with a median initially of 390 and finally of 485 for the Chao1 alpha diversity metric of the samples, respectively (Fig. 5. A). The metrics observed OTUs and Faith's phylogenetic diversity showed a similar trend (Fig. S2). Dominant microorganisms included bacteria belonging to the *Clostridium* genus and the families Pseudomonadaceae, Thermovirgaceae and uncultured ML1228J-1 (Fig. 6.). *Clostridium* species and members of the Pseudomonadaceae have been found to anaerobically degrade phenol (Lack and Fuchs, 1994; Zhang and Wiegel, 1994). Bacteria belonging to Thermovirgaceae may be related to the degradation of phenolic compounds (DiPippo et al., 2009). The family of uncultured ML1228J-1 is associated with anoxic and saline conditions (Humayoun et al., 2003). Archaea present in the start-up phase included the dominating hydrogenotrophic methanogens belonging to the *Methanobacterium* genus and acetoclastic *Methanosaeta* genus (Fig. 6).

In phase II, the phenol concentration was increased. Alpha diversity showed further adaptation of the microbial community to phenol with an initial decrease and subsequent increase of the diversity (Fig. 5. A). The relative abundance of *Clostridium* species increased (to 19%) while the relative abundance of members of Pseudomonadaceae slightly reduced and Mogibacteriaceae became more dominant in phase II. Mogibacteriaceae are anaerobic Gram-positive bacteria that have been found in anaerobic digestion processes and of which the function in the reactor is unclear (da Silva Martins et al., 2017). Other microorganisms, bacteria belonging to the order BA021, were dominating more prominently at the beginning of phase II but were also present throughout the entire experiment (in relative abundances from 21 to 2%). The order BA021 is part of the OP9 and JS1 lineages (Fig. S3). These lineages are also referred to as Atribacteria and may be thriving using a syntrophic metabolism (Nobu et al., 2015). Archaeal species dominating in this phase belonged to the *Methanobacterium* and *Methanosaeta* genus (Fig. 6.).

Sodium concentration was increased in phase III, and the alpha diversity of the overall microbial community showed an increase (from a Chao1 median of 421–517, see Fig. 5. A), which may indicate that the microbial community was likely influenced by the increased salinity. Members of the Pseudomonadaceae increased in relative abundance from 1 to 20%, while the ML1228J-1 and Mogibacteriaceae families decreased to an abundance of 1% (Fig. 6.).

A definite decrease in alpha diversity was observed in phase IV when the sodium was changed to 16 $gNa^{+}.L^{-1}$ (median of the Chao1 metric was 261) (Fig. 5. A). In general, Gram-positive bacteria and archaea can better tolerate salinity changes because of the strong cell wall (Yan et al., 2015). Salinity is known to enrich for salt-tolerant and halophilic bacteria in membrane bioreactors and other anaerobic reactors (Luo et al., 2016; Wang et al., 2017a). Decreases in relative abundances were observed for the Gram-negative Pseudomonadaceae, where salt-tolerant Thermovirgaceae and Gram-positive Clostridium species were highly abundant (26% and 31%, respectively). Among the archaea, the hydrogenotrophic *Methanobacterium* species became more dominant (Fig. 6). The dominance of *Methanobacterium* and *Methanosaeta* was described in a UASB reactor operated under high salinity, and although the *Methanosaeta* species were dominant, they do not have a very high salt tolerance (Onodera et al., 2017). Possibly, the presence of *Methanosaeta* is crucial for granule formation in UASB reactors, but in the AnMBR, these species may be less essential, and hydrogenotrophic *Methanobacterium* are also dominant. Madigou et al. (2016) also indicated the importance of hydrogenotrophic methanogenesis at high phenol concentrations. During the temporary lowering of the OLR, the community alpha diversity increased indicating a recovery of the microbial diversity (Chao1 median of 356). *Clostridium* species highly dominated among bacteria (54%). Furthermore, among archaea, the relative abundance of *Methanosaeta* increased (from 1 to 10%) and of *Methanobacterium* decreased (from 20 to 5%, Fig. 6.).

Alpha diversity did not reach similar high values as before phase IV (with Chao1 index medians of 438 and 386 for phase V and VI, respectively). However, the alpha diversities were similar, indicating that the microbial community was more tolerant to fluctuating salinity (Fig. 5. A). Accordingly, the community composition in phase V and VI was very similar with *Clostridium*, Thermovirgaceae as well as ML1228J-1 as dominating bacteria and *Methanobacterium* and *Methanosaeta* as main archaea (Fig. 6.).

Beta diversity or between-sample diversity was determined to illustrate the influence of the salinity on the microbial community diversity. In the NMDS plot, samples from the start-up phase I seemed to cluster separately from the phases II to IV in which phenol or sodium concentration was changed (Fig. 5. B). However, this could not be confirmed by the PCoA analysis (Fig. 5. C). Together, the beta diversity plots indicated a gradual change in the community diversity although this did not result in differences in the clustering. Samples from the final phases V and VI in which the reactors were operated with short-term salinity changes, were not clustering with any of the samples from phases I to IV (Fig. 5. B, C). The microbial community could have responded in different ways to disturbances in phenol and sodium concentration from the ecological point-of-view (Shade et al., 2012). Although sodium concentration fluctuated in phase V and VI, the community diversity remained more similar compared to previous phases. Given the similar microbial community diversity and profile as well as efficient bioreactor performance in phase V and VI, a gradual adaptation to environmental conditions increased the resistance of the microbial community to sodium fluctuations, which increased the robustness of the AnMBR system.

3.4.1. Phenol-degrading bacteria in the AnMBR

Clostridium has been identified as dominating and was possibly related to phenol degradation in the AnMBR. *Clostridium hydroxybenzoicum* can transform phenol to 4-hydroxybenzoate (Zhang and Wiegel, 1994), and *Clostridium* strain 6 enhanced phenol degradation when growing in coculture (Letowski et al., 2001). In a UASB reactor treating phenolic wastewater at high salinity, increased phenolics concentrations increased the relative abundance of Clostridia (Wang et al., 2017b). Additionally, anaerobic phenol degradation could occur via syntrophic conversions. However, the role of syntrophic microorganisms in anaerobic digestion is yet poorly understood, and the relationship between the so-called microbial dark matter with syntrophy remains unclear

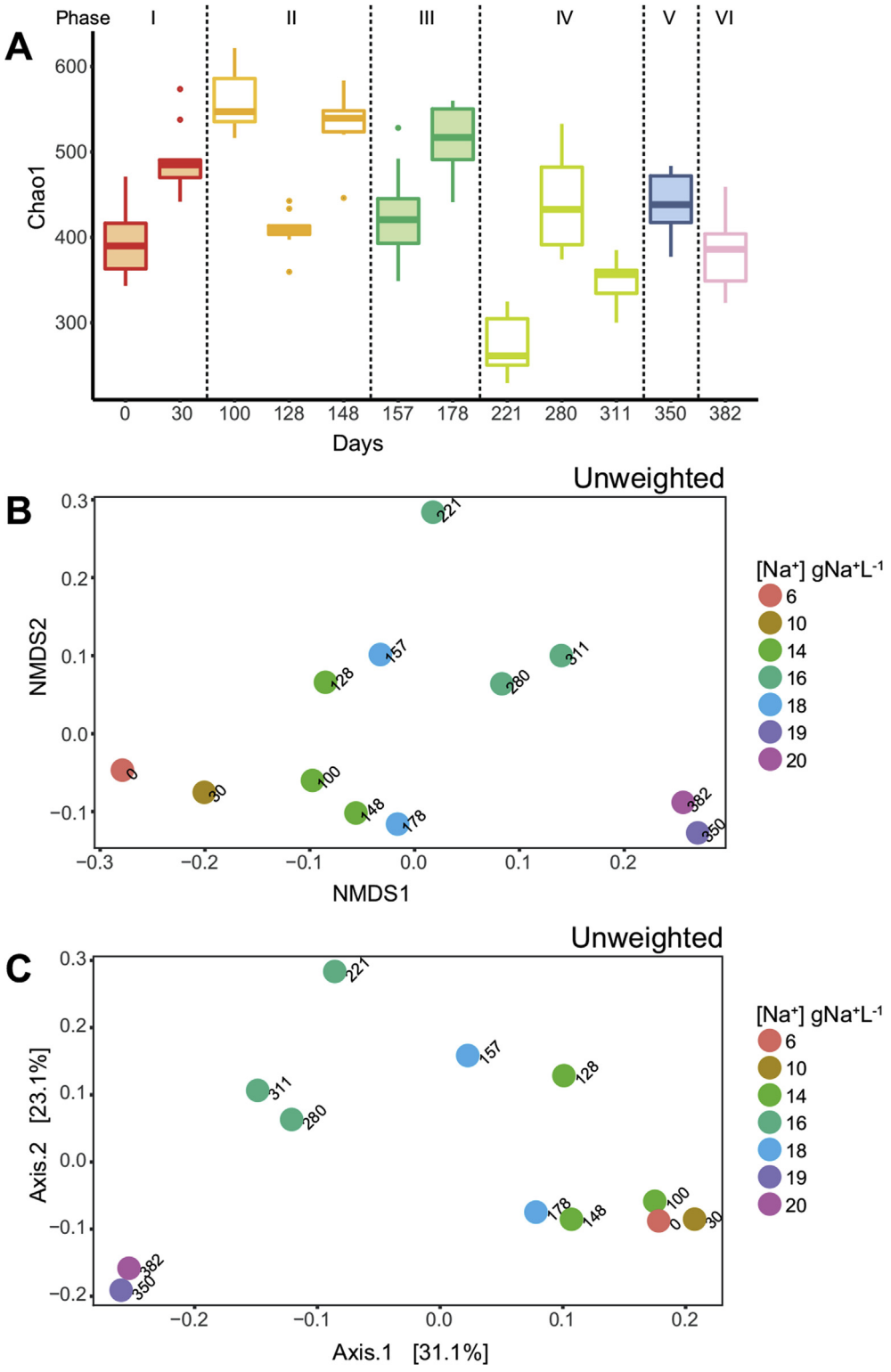

Fig. 5. Diversity plots for the microbial community in AnMBR. Plots present for different phases of operation the alpha diversity (Chao1 metric) (A), for different sodium concentrations the NMDS beta diversity based on unweighted Unifrac values (B) and the PCoA analysis of unweighted Unifrac values (C).

(Narihiro et al., 2015). However, in an attempt to shed some light on possible syntrophic microorganisms, the low abundant taxa (relative abundance below 1%) were studied, and among them, syntrophic phenol degraders could be identified. These included bacteria related to the genera *Desulfotomaculum, Syntrophus, Desulfovibrio, Syntrophorhabdus, and Pelotomaculum,* among others (Fig. 7.). *Desulfovibrio* was identified in a phenol-degrading and biogas-producing reactor (Ju and Zhang, 2014). *Syntrophorhabdus* was found in a phenolic-degrading UASB reactor at high salinity (Wang et al., 2017b). *Syntrophorhabdus aromaticivorans* strain UI

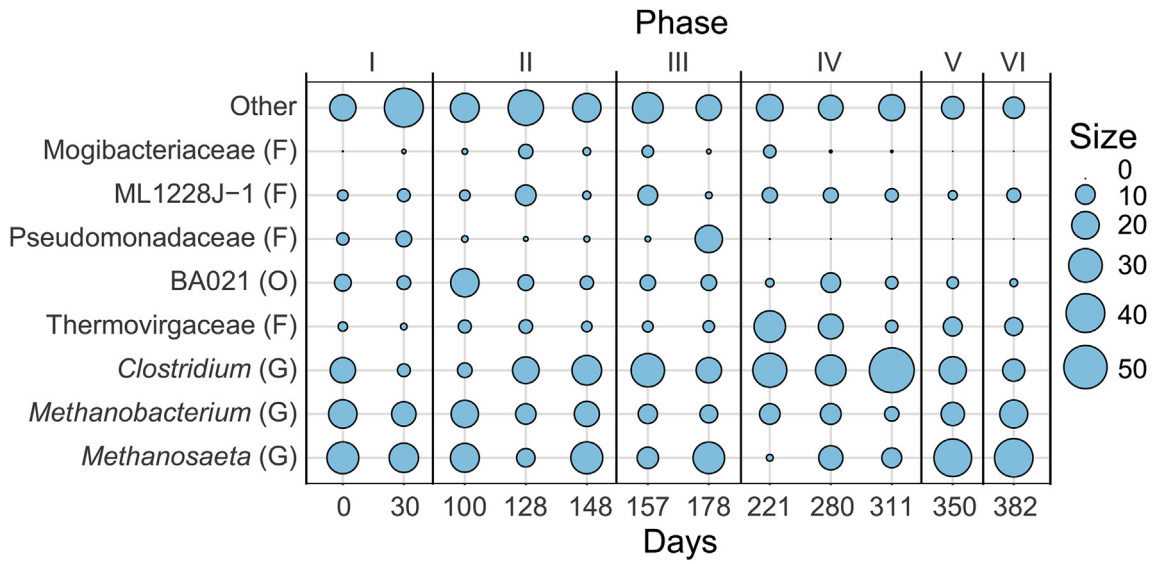

Fig. 6. Microbial community composition of the AnMBR treating high salinity phenolic wastewater according to the most detailed level of taxonomy that could be inferred from the OTU sequences. Relative abundance cut-off at 5%.

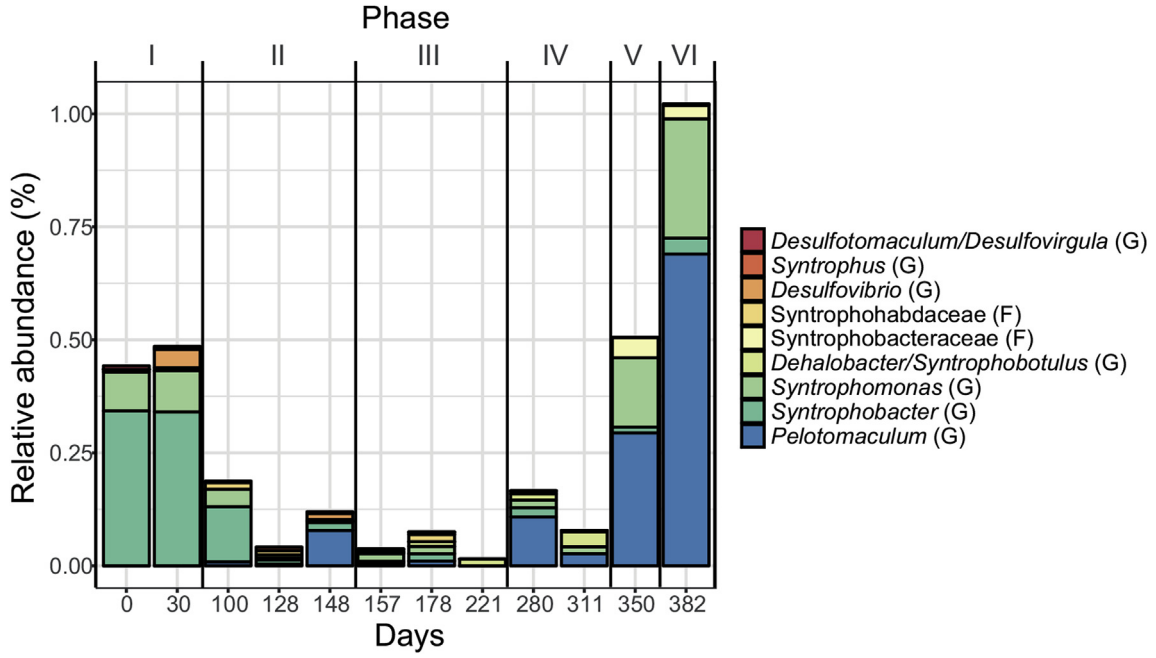

Fig. 7. Relative abundance of taxa related to syntrophic phenol degradation that are present in the AnMBR.

was the first isolated syntrophic phenol degrader (Qiu et al., 2008) via benzoate as intermediate (Nobu et al., 2014). *Pelotomaclum* species were shown to syntrophically degrade aromatic compounds (Qiu et al., 2006). *Desulfotomaculum, Syntrophus,* and *Pelotomaculum* were identified in phenol-containing wastewater (Chen et al., 2008). Moreover, *Syntrophus, Syntrophorhabdus,* and *Pelotomaculum* were identified in lab- and full-scale reactors treating aromatics containing wastewater (Nobu et al., 2017). In this study, the syntrophic phenol-degraders were observed in the start-up phase I, decreased during the long-term phases II and III and increased in phases IV to VI, likely indicating the establishment of this functional group of phenol degraders (Fig. 7.). *Pelotomaculum* showed an evident increase in relative abundance when the microbial community was adapted to sodium fluctuations and exhibited maximum phenol conversion rates.

4. Conclusions

The conclusions drawn from the present work can be summarized as follows:

- Salinity was increased from 8 to 20 $gNa^{+}.L^{-1}$ during long-term operation of the AnMBR reactor. Phenol removal efficiency of 99.9% was achieved at 14 $gNa^{+}.L^{-1}$. Phenol conversion rates increased from 5.1 $mgPh.gVSS^{-1}.d^{-1}$ at 16 $gNa^{+}.L^{-1}$ to a maximum conversion rate of 11.7 $mgPh.gVSS^{-1}.d^{-1}$ at 20

$gNa^+.L^{-1}$. Adaptation of the microbial community to salinity changes promoted a higher removal efficiency of phenol. The specific methanogenic activity decreased by 24% when the Na^+ concentration increased from 14 to 20 $gNa^+.L^{-1}$.

- A one-step salinity increase from 14 to 18 $gNa^+.L^{-1}$ compromised 21.2% of the cells membranes, reducing the quality, and biological stability of the biomass. However, the AnMBR overall conversion performance was not affected by a short-term stepwise 2 $gNa^+.L^{-1}$ salinity fluctuations inside the reactor. The process exhibited robustness and strengthened microbial community to salinity changes in the range of concentrations applied.
- Membrane filtration was adversely affected by the salinity increase, which was exhibited by an increasing transmembrane pressure to about 350 mbar, and concomitantly the membrane filtration resistance increase was attributed to a ten-fold reduction on biomass particle size from 185 μm at 14 $gNa^+.L^{-1}$ to 16 μm at 20 $gNa^+.L^{-1}$.
- Batch tests demonstrated that COD removal and methane production rates for the 0.03, 0.025, 0.02 K^+:Na^+ ratios were found to be lower than for the 0.05 K^+:Na^+ ratio. However, phenol removal was lower at 24 $gNa^+.L^{-1}$ compared to 16 and 20 $gNa^+.L^{-1}$.
- Bacteria belonging to the *Clostridium* genus (up to 54% relative abundance) dominated the bacterial community and archaea were dominated by *Methanobacterium* and *Methanosaeta* genus. Syntrophic phenol-degrading bacteria, such as *Pelotomaculum* showed an increased relative abundance after adaptation of the microbial community to salinity changes in combination with higher phenol degradation.

Acknowledgements

This research is supported by the Dutch Technology Foundation (STW, Project No.13348), which is part of the Netherlands Organization for Scientific Research (NWO), partly funded by the Dutch Ministry of Economic Affairs. This research is co-sponsored by Evides Industriewater and Paques B.V. The authors thank the intern student Basak Donmez for helping with laboratory analysis during the last two phases of this study.

Appendix A. Supplementary data

Supplementary data related to this article can be found at https://doi.org/10.1016/j.watres.2018.05.006.

References

Abou-Elela, S.I., Kamel, M.M., Fawzy, M.E., 2010. Biological treatment of saline wastewater using a salt-tolerant microorganism. Desalination 250 (1), 1–5.
Aslan, S., Şekerdağ, N., 2016. Salt inhibition on anaerobic treatment of high salinity wastewater by upflow anaerobic sludge blanket (UASB) reactor. Desalination Water Treat. 57 (28), 12998–13004.
Caporaso, J.G., Kuczynski, J., Stombaugh, J., Bittinger, K., Bushman, F.D., Costello, E.K., Fierer, N., Pena, A.G., Goodrich, J.K., Gordon, J.I., Huttley, G.A., Kelley, S.T., Knights, D., Koenig, J.E., Ley, R.E., Lozupone, C.A., McDonald, D., Muegge, B.D., Pirrung, M., Reeder, J., Sevinsky, J.R., Turnbaugh, P.J., Walters, W.A., Widmann, J., Yatsunenko, T., Zaneveld, J., Knight, R., 2010. QIIME allows analysis of high-throughput community sequencing data. Br. J. Pharmacol. 7 (5), 335–336.
Carballa, M., Regueiro, L., Lema, J.M., 2015. Microbial management of anaerobic digestion: exploiting the microbiome-functionality nexus. Curr. Opin. Biotechnol. 33 (Suppl. C), 103–111.
Chen, C.-L., Wu, J.-H., Liu, W.-T., 2008. Identification of important microbial populations in the mesophilic and thermophilic phenol-degrading methanogenic consortia. Water Res. 42 (8), 1963–1976.
Chen, L., Gu, Y., Cao, C., Zhang, J., Ng, J.-W., Tang, C., 2014. Performance of a submerged anaerobic membrane bioreactor with forward osmosis membrane for low-strength wastewater treatment. Water Res. 50, 114–123.
da Silva Martins, A., Ornelas Ferreira, B., Ribeiro, N.C., Martins, R., Rabelo Leite, L., Oliveira, G., Colturato, L.F., Chernicharo, C.A., de Araujo, J.C., 2017. Metagenomic analysis and performance of a mesophilic anaerobic reactor treating food waste at various load rates. Environ. Technol. 38 (17), 2153–2163.
De Vrieze, J., Christiaens, M.E.R., Walraedt, D., Devooght, A., Ijaz, U.Z., Boon, N., 2017. Microbial community redundancy in anaerobic digestion drives process recovery after salinity exposure. Water Res. 111, 109–117.
DiPippo, J.L., Nesbø, C.L., Dahle, H., Doolittle, W.F., Birkland, N.-K., Noll, K.M., 2009. Kosmotoga olearia gen. nov., sp. nov., a thermophilic, anaerobic heterotroph isolated from an oil production fluid. Int. J. Syst. Evol. Microbiol. 59 (12), 2991–3000.
Edgar, R., 2016. UCHIME2: Improved Chimera Prediction for Amplicon Sequencing (bioRxiv).
Edgar, R.C., 2010. Search and clustering orders of magnitude faster than BLAST. Bioinformatics 26 (19), 2460–2461.
Gagliano, M.C., Ismail, S.B., Stams, A.J.M., Plugge, C.M., Temmink, H., Van Lier, J.B., 2017. Biofilm formation and granule properties in anaerobic digestion at high salinity. Water Res. 121, 61–71.
Hemmelmann, A., Torres, A., Vergara, C., Azocar, L., Jeison, D., 2013. Application of anaerobic membrane bioreactors for the treatment of protein-containing wastewaters under saline conditions. J. Chem. Technol. Biotechnol. 88 (4), 658–663.
Humayoun, S.B., Bano, N., Hollibaugh, J.T., 2003. Depth distribution of microbial diversity in mono lake, a meromictic soda lake in California. Appl. Environ. Microbiol. 69 (2), 1030–1042.
Hussain, A., Dubey, S.K., 2014. Specific methanogenic activity test for anaerobic treatment of phenolic wastewater. Desalination Water Treat. 52 (37–39), 7015–7025.
Ismail, S.B., de La Parra, C.J., Temmink, H., van Lier, J.B., 2010. Extracellular polymeric substances (EPS) in upflow anaerobic sludge blanket (UASB) reactors operated under high salinity conditions. Water Res. 44 (6), 1909–1917.
Ismail, S.B., Gonzalez, P., Jeison, D., Van Lier, J.B., 2008. Effects of High Salinity Wastewater on Methanogenic Sludge Bed Systems, pp. 1963–1970.
Jeison, D., Del Rio, A., Van Lier, J.B., 2008a. Impact of High Saline Wastewaters on Anaerobic Granular Sludge Functionalities, pp. 815–819.
Jeison, D., Kremer, B., van Lier, J.B., 2008b. Application of membrane enhanced biomass retention to the anaerobic treatment of acidified wastewaters under extreme saline conditions. Separ. Purif. Technol. 64 (2), 198–205.
Ju, F., Zhang, T., 2014. Novel microbial populations in ambient and mesophilic biogas-producing and phenol-degrading consortia unraveled by high-throughput sequencing. Microb. Ecol. 68 (2), 235–246.
Kuo, M.M.C., Haynes, W.J., Loukin, S.H., Kung, C., Saimi, Y., 2005. Prokaryotic K+ channels: from crystal structures to diversity. FEMS (Fed. Eur. Microbiol. Soc.) Microbiol. Rev. 29 (5), 961–985.
Lack, A., Fuchs, G., 1994. Evidence that phenol phosphorylation to phenylphosphate is the first step in anaerobic phenol metabolism in a denitrifying Pseudomonas sp. Arch. Microbiol. 161 (2), 132–139.
Le Borgne, S., Paniagua, D., Vazquez-Duhalt, R., 2008. Biodegradation of organic pollutants by halophilic bacteria and archaea. J. Mol. Microbiol. Biotechnol. 15 (2–3), 74–92.
Lefebvre, O., Quentin, S., Torrijos, M., Godon, J.J., Delgenès, J.P., Moletta, R., 2007. Impact of increasing NaCl concentrations on the performance and community composition of two anaerobic reactors. Appl. Microbiol. Biotechnol. 75 (1), 61–69.
Letowski, J., Juteau, P., Villemur, R., Duckett, M.-F., Beaudet, R., Lépine, F., Bisaillon, J.-G., 2001. Separation of a phenol carboxylating organism from a two-member, strict anaerobic co-culture. Can. J. Microbiol. 47 (5), 373–381.
Luo, W., Phan, H.V., Hai, F.I., Price, W.E., Guo, W., Ngo, H.H., Yamamoto, K., Nghiem, L.D., 2016. Effects of salinity build-up on the performance and bacterial community structure of a membrane bioreactor. Bioresour. Technol. 200 (Suppl. C), 305–310.
Madigou, C., Poirier, S., Bureau, C., Chapleur, O., 2016. Acclimation strategy to increase phenol tolerance of an anaerobic microbiota. Bioresour. Technol. 216 (Suppl. C), 77–86.
Margesin, R., Schinner, F., 2001. Potential of halotolerant and halophilic microorganisms for biotechnology. Extremophiles 5 (2), 73–83.
McDonald, D., Price, M.N., Goodrich, J., Nawrocki, E.P., Desantis, T.Z., Probst, A., Andersen, G.L., Knight, R., Hugenholtz, P., 2012. An improved Greengenes taxonomy with explicit ranks for ecological and evolutionary analyses of bacteria and archaea. ISME J. 6 (3), 610–618.
McMurdie, P.J., Holmes, S., 2013. Phyloseq: an R package for reproducible interactive analysis and graphics of microbiome census data. PLoS One 8 (4).
Muñoz Sierra, J.D., Lafita, C., Gabaldón, C., Spanjers, H., van Lier, J.B., 2017. Trace metals supplementation in anaerobic membrane bioreactors treating highly saline phenolic wastewater. Bioresour. Technol. 234, 106–114.
Narihiro, T., Nobu, M.K., Kim, N.-K., Kamagata, Y., Liu, W.-T., 2015. The nexus of syntrophy-associated microbiota in anaerobic digestion revealed by long-term enrichment and community survey. Environ. Microbiol. 17 (5), 1707–1720.
Ng, H.Y., Ong, S.L., Ng, W.J., 2005. Effects of sodium chloride on the performance of a sequencing batch reactor. J. Environ. Eng. 131 (11), 1557–1564.
Nobu, M.K., Dodsworth, J.A., Murugapiran, S.K., Rinke, C., Gies, E.A., Webster, G., Schwientek, P., Kille, P., Parkes, R.J., Sass, H., Jørgensen, B.B., Weightman, A.J., Liu, W.-T., Hallam, S.J., Tsiamis, G., Woyke, T., Hedlund, B.P., 2015. Phylogeny and physiology of candidate phylum 'Atribacteria' (OP9/JS1) inferred from cultivation-independent genomics. ISME J. 10, 273.
Nobu, M.K., Narihiro, T., Liu, M., Kuroda, K., Mei, R., Liu, W.-T., 2017. Thermodynamically diverse syntrophic aromatic compound catabolism. Environ.

Microbiol. 19 (11), 4576–4586.
Nobu, M.K., Narihiro, T., Tamaki, H., Qiu, Y.-L., Sekiguchi, Y., Woyke, T., Goodwin, L., Davenport, K.W., Kamagata, Y., Liu, W.-T., 2014. Draft genome sequence of Syntrophorhabdus aromaticivorans strain UI, a mesophilic aromatic compound-degrading syntroph. Genome Announc. 2 (1) e01064–01013.
Onodera, T., Syutsubo, K., Hatamoto, M., Nakahara, N., Yamaguchi, T., 2017. Evaluation of cation inhibition and adaptation based on microbial activity and community structure in anaerobic wastewater treatment under elevated saline concentration. Chem. Eng. J. 325, 442–448.
Pevere, A., Guibaud, G., van Hullebusch, E.D., Boughzala, W., Lens, P.N.L., 2007. Effect of Na+ and Ca2+ on the aggregation properties of sieved anaerobic granular sludge. Colloid. Surface. Physicochem. Eng. Aspect. 306 (1–3 SPEC. ISS.), 142–149.
Poirier, S., Bize, A., Bureau, C., Bouchez, T., Chapleur, O., 2016. Community shifts within anaerobic digestion microbiota facing phenol inhibition: towards early warning microbial indicators? Water Res. 100 (Suppl. C), 296–305.
Praveen, P., Nguyen, D.T.T., Loh, K.-C., 2015. Biodegradation of phenol from saline wastewater using forward osmotic hollow fiber membrane bioreactor coupled chemostat. Biochem. Eng. J. 94 (Suppl. C), 125–133.
Prest, E.I., Hammes, F., Kötzsch, S., van Loosdrecht, M.C.M., Vrouwenvelder, J.S., 2013. Monitoring microbiological changes in drinking water systems using a fast and reproducible flow cytometric method. Water Res. 47 (19), 7131–7142.
Qiu, Y.-L., Hanada, S., Ohashi, A., Harada, H., Kamagata, Y., Sekiguchi, Y., 2008. Syntrophorhabdus aromaticivorans gen. Nov., sp. nov., the first cultured anaerobe capable of degrading phenol to acetate in obligate syntrophic associations with a hydrogenotrophic methanogen. Appl. Environ. Microbiol. 74 (7), 2051–2058.
Qiu, Y.-L., Sekiguchi, Y., Hanada, S., Imachi, H., Tseng, I.-C., Cheng, S.-S., Ohashi, A., Harada, H., Kamagata, Y., 2006. Pelotomaculum terephthalicum sp. nov. and Pelotomaculum isophthalicum sp. nov.: two anaerobic bacteria that degrade phthalate isomers in syntrophic association with hydrogenotrophic methanogens. Arch. Microbiol. 185 (3), 172–182.
Shade, A., Peter, H., Allison, S.D., Baho, D.L., Berga, M., Bürgmann, H., Huber, D.H., Langenheder, S., Lennon, J.T., Martiny, J.B.H., Matulich, K.L., Schmidt, T.M., Handelsman, J., 2012. Fundamentals of microbial community resistance and resilience. Front. Microbiol. 3, 417.
Song, X., McDonald, J., Price, W.E., Khan, S.J., Hai, F.I., Ngo, H.H., Guo, W., Nghiem, L.D., 2016. Effects of salinity build-up on the performance of an anaerobic membrane bioreactor regarding basic water quality parameters and removal of trace organic contaminants. Bioresour. Technol. 216 (Suppl. C), 399–405.
Sudmalis, D., Gagliano, M.C., Pei, R., Grolle, K., Plugge, C.M., Rijnaarts, H.H.M., Zeeman, G., Temmink, H., 2018. Fast anaerobic sludge granulation at elevated salinity. Water Res. 128 (Suppl. C), 293–303.
van Lier, J.B., van der Zee, F.P., Frijters, C.T.M.J., Ersahin, M.E., 2015. Celebrating 40 years anaerobic sludge bed reactors for industrial wastewater treatment. Rev. Environ. Sci. Biotechnol. 14 (4), 681–702.
Vyrides, I., Stuckey, D.C., 2009a. Effect of fluctuations in salinity on anaerobic biomass and production of soluble microbial products (SMPs). Biodegradation 20 (2), 165–175.
Vyrides, I., Stuckey, D.C., 2009b. Saline sewage treatment using a submerged anaerobic membrane reactor (SAMBR): effects of activated carbon addition and biogas-sparging time. Water Res. 43 (4), 933–942.
Vyrides, I., Stuckey, D.C., 2011. Fouling cake layer in a submerged anaerobic membrane bioreactor treating saline wastewaters: curse or a blessing? Water Sci. Technol. 63 (12), 2902–2908.
Vyrides, I., Stuckey, D.C., 2017. Compatible solute addition to biological systems treating waste/wastewater to counteract osmotic and other environmental stresses: a review. Crit. Rev. Biotechnol. 37 (7), 865–879.
Wang, S., Hou, X., Su, H., 2017a. Exploration of the relationship between biogas production and microbial community under high salinity conditions. Sci. Rep. 7 (1).
Wang, W., Wu, B., Pan, S., Yang, K., Hu, Z., Yuan, S., 2017b. Performance robustness of the UASB reactors treating saline phenolic wastewater and analysis of microbial community structure. J. Hazard Mater. 331 (Suppl. C), 21–27.
Wang, W., Yang, K., Muñoz Sierra, J., Zhang, X., Yuan, S., Hu, Z., 2017c. Potential impact of methyl isobutyl ketone (MIBK) on phenols degradation in an UASB reactor and its degradation properties. J. Hazard Mater. 333 (Suppl. C), 73–79.
Wood, J.M., 2015. Bacterial responses to osmotic challenges. J. Gen. Physiol. 145 (5), 381–388.
Woolard, C.R., Irvine, R.L., 1995. Treatment of hypersaline wastewater in the sequencing batch reactor. Water Res. 29 (4), 1159–1168.
Wu, Y., Wang, X., Tay, M.Q.X., Oh, S., Yang, L., Tang, C., Cao, B., 2017. Metagenomic insights into the influence of salinity and cytostatic drugs on the composition and functional genes of microbial community in forward osmosis anaerobic membrane bioreactors. Chem. Eng. J. 326, 462–469.
Yan, N., Marschner, P., Cao, W., Zuo, C., Qin, W., 2015. Influence of salinity and water content on soil microorganisms. Int. Soil Water Conserv. Res. 3 (4), 316–323.
Yang, J., Spanjers, H., Jeison, D., Van Lier, J.B., 2013. Impact of Na+ on biological wastewater treatment and the potential of anaerobic membrane bioreactors: a review. Crit. Rev. Environ. Sci. Technol. 43 (24), 2722–2746.
Yang, J., Tian, Z., Spanjers, H., Van Lier, J.B., 2014. Feasibility of using NaCl to reduce membrane fouling in anaerobic membrane bioreactors. Water Environ. Res. 86 (4), 340–345.
Yogalakshmi, K.N., Joseph, K., 2010. Effect of transient sodium chloride shock loads on the performance of submerged membrane bioreactor. Bioresour. Technol. 101 (18), 7054–7061.
Yurtsever, A., Calimlioglu, B., Görür, M., Çinar, Ö., Sahinkaya, E., 2016. Effect of NaCl concentration on the performance of sequential anaerobic and aerobic membrane bioreactors treating textile wastewater. Chem. Eng. J. 287, 456–465.
Zhang, X., Wiegel, J., 1994. Reversible conversion of 4-hydroxybenzoate and phenol by Clostridium hydroxybenzoicum. Appl. Environ. Microbiol. 60 (11), 4182–4185.